Indonesian Journal of Chemical Research

http://ojs3.unpatti.ac.id/index.php/ijcr Indo. J. Chem. Res., 14 (1), 77-87, 2026

Evaluation of 5,5'-Oxybis(1,3,7-Trihydroxy-9H-Xanthen-9-One) as an Anticancer Agent Through *In Vitro* and *In Silico* Tests

Ayu Nadila Safitri[1*], Aldillah Herlambang[2], Muhammad Irhash Shalihin[1], Nurul Pratiwi[1], Putri Dwi Mulyani[3], Nania Septiyani[1], Muktaf Wando Saputra[1]

[1] Chemistry Program, Department of Mathematics and Natural Sciences, Faculty of Sciences and Technology, Universitas Jambi, Jambi 36361, Indonesia

[2] Chemical Engineering Program, Department of Civil, Chemical and Environmental Engineering, Faculty of Sciences and Technology, Universitas Jambi, Jambi 36361, Indonesia

[3] Biology Program, Department of Mathematics and Natural Sciences, Faculty of Sciences and Technology, Universitas Jambi, Jambi 36361, Indonesia

[*]*Corresponding Author: ayunadilasafitri@unja.ac.id*

Received: January 2026
Received in revised: April 2026
Accepted: May 2026
Available online: May 2026

Abstract

Breast cancer is among the most common malignancies globally and continues to be a primary cause of cancer-related deaths in women. Modern chemotherapeutic agents often exhibit resistance and lack of selectivity for healthy cells, leading to significant side effects. Consequently, several strategies are essential to overcome resistance and enhance the selectivity and efficacy of chemotherapeutic drugs derived from natural sources. This study investigates the anticancer activity of a new bis-xanthone compound, 5,5'-Oxybis(1,3,7-trihydroxy-9H-xanthen-9-one), in MCF-7 breast cancer cells using a combination of in vitro and in silico approaches. The compound exhibited cytotoxicity against MCF-7 breast cancer cells, with an IC_{50} value of 30.47 µg/mL. The pharmacokinetic characteristics of bis-xanthone compounds were evaluated using absorption, distribution, metabolism, excretion, and toxicity (ADMET) tests, demonstrating a more favorable profile than that of doxorubicin, a standard anticancer drug.

Keywords: Anticancer, Xanthone, MCF-7, Chemotherapeutic agent, in vitro, in silico

INTRODUCTION

Globally, Breast malignancy represents the second most prevalent and fatal oncological condition, disproportionately striking female populations (Siegel et al., 2017). Annual epidemiological indices indicate that this pathology constitutes roughly 30% of all newly diagnosed female oncological cases (Bai et al., 2018). Structurally, these neoplasms predominantly arise within the ductal epithelium, with a pronounced risk of progression to invasive ductal carcinoma. Historical clinical registries underscore the profound lethality of malignant diseases; out of 348,809 recorded medical instances in 2018, approximately 16.7% were directly linked to mammary carcinomas. Within the Indonesian demographic, mammary and cervical carcinomas emerge as the leading oncological threats. Mechanistically, carcinogenesis is driven by aberrant, unchecked cellular proliferation that progressively disrupts systemic physiological and organic operations. This specific risk trajectory scales concurrently with advanced age in women. Clinical management traditionally relies on systemic chemotherapy, an intervention frequently complicated by toxicities like emesis, peripheral neuropathic damage, and myelosuppression (Hasanah et al., 2026). Globally, it precipitates roughly 670,000 fatalities out of 2.3 million diagnosed patients. Beyond ductal origins, oncogenesis can similarly initiate within the specialized epithelial lining of lobular ductules and acini, or even within supportive stromal architecture (Tipaheuw et al., 2025). Within standard protocols, the anthracycline doxorubicin remains a foundational therapeutic agent (Hermawan et al., 2010). However, its clinical utility is severely limited by systemic cytotoxicity and profound hazards to non-malignant tissue (Kurniawan, 2025).

Consequently, botanical derivatives have garnered significant attention as highly selective, efficacious alternatives that mitigate toxic side effects (Amir & Murcitro, 2017). Plants such as the mangosteen are characterized by an extensive profile of secondary metabolites, specifically complex

xanthone derivatives including mangostin, mangostenol, mangostinon A and B, trapezifolixanthone, tovophyllin B, alpha- and beta-mangostin, garcinon B, mangostanol, epicatechin, diverse flavonoids, and gartanin. These principal bioactive xanthones are highly concentrated within the pericarp and are renowned for their robust radical-scavenging capabilities (Kalkoy et al., 2025). Chemically defined as an oxygenated heterocyclic core structure designated 9H-xanthen-9-one (Kurniawan, 2025), xanthones exhibit a broad spectrum of therapeutic applications, encompassing documented antioxidant, anti-inflammatory, antimicrobial, antiviral, anti-retroviral, and distinct antineoplastic properties (Darwati et al., 2021).

Prior investigations demonstrate that chemical constituents sourced from the Garcinia genus display pronounced antineoplastic properties. Specifically, garcisanton B and C isolated from G. mangostana have demonstrated robust cytotoxic efficacy against mammary adenocarcinoma cells (MCF-7), yielding IC_{50} values of 4.27 and 2.65 µg/mL, respectively (Mohamed & Ibrahim, 2022). Recently, Safitri et al. (2020) successfully elucidated and isolated a novel terpolyoxygenated xanthone dimer, chemically identified as 5,5'-Oxybis(1,3,7-trihydroxy-9H-xanthen-9-one), as cataloged in the supplementary scientific records. However, following its initial isolation, the specific pharmacological profile and bioactivity of this dimeric molecule have remained completely unexplored. This omission represents a critical gap in the current oncological literature, as determining both cytotoxic thresholds and precise cellular pathways is mandatory for downstream pharmaceutical translation.

The MCF-7 cellular lineage serves as the primary experimental paradigm for this investigation, representing an estrogen receptor-positive (ER+) mammary carcinoma model heavily utilized in antineoplastic discovery due to its clinical relevance in predicting patient therapeutic responses. Consequently, this study evaluates the antineoplastic potential of the isolated dimer against MCF-7 cells utilizing an integrated in vitro and in silico investigative framework. The in vitro assays quantify direct cell death kinetics, whereas the in silico simulations model molecular binding topologies and predict underlying biological receptors, thereby mapping the potential mechanism of action.

The novelty of this project lies in the inaugural comprehensive characterization of this dimeric xanthone's antineoplastic properties, thereby expanding the library of viable lead structures derived from botanical sources. Ultimately, unifying laboratory phenotypic screens with predictive computational modeling is anticipated to provide deeper insights regarding the compound's target selectivity, therapeutic window, and safety profile for breast cancer intervention.

METHODOLOGY

Materials and Instrumentals

Human mammary cancer cells, especially the MCF-7 ATCC-HBT-22TM lineage, were tested in this experimental framework against pure separated fractions of the dimeric xanthone derivative 5,5'-Oxybis(1,3,7-trihydroxy-9H-xanthen-9-one.
Researchers used the tetrazolium dye MTT ($C_{18}H_{17}N_5S$) in conjunction with Roswell Park Memorial Institute (RPMI) 1640 growth substrate for the required in vitro cytotoxicity screenings. The substrate was routinely supplemented with 10% Foetal Bovine Serum (Gibco), 2% penicillin-streptomycin antibiotic cocktail, and 0.5% Fungizone (Gibco) to ensure the culture was as sterile as possible.

Methods

In Vitro Evaluation of the Anticancer Activity of Xanthone Compound

The colorimetric 3-[4,5-dimethylthiazol-2-yl]-2,5-diphenyltetrazolium-bromide (MTT) metabolic test was used to assess the xanthone derivative's antineoplastic activity quantitatively. Within 96-well microplates containing RPMI growth medium supplemented with 10% foetal bovine serum and 1% penicillin-streptomycin, cellular cultures were extended. These prepared plates were subsequently maintained under controlled conditions at 37°C for an initial 24-hour equilibration period. Following this stabilization phase, the experimental xanthone monomer was dispensed into the designated cellular wells across a serial dilution gradient of 1000, 500, 250, 125, 62.5, 31.25, 15.625, and 7.8125 µg/mL, after which the exposed cells were maintained for a prolonged 48-hour exposure interval. Upon completion of this treatment window, standard MTT solution was pipetted into each microplate well, and the plate was incubated for 4 hours. Cellular survival rates were directly determined via monitoring mitochondrial metabolic activity. In particular, the yellow tetrazolium salt is transformed into insoluble, purple-colored formazan crystals by active mitochondrial dehydrogenases in live cells. These crystalline structures were subsequently dissolved by adding a dimethyl sulfoxide (DMSO) solubilization agent. Optical density measurements were systematically

captured using an Enzyme-Linked Immunosorbent Assay (ELISA) microplate reader at 450 nm. The overall cytotoxic potency is quantified by the half-maximal inhibitory concentration (IC50), which was computed by linear regression.

In Silico Evaluation of the Anticancer Activity of Xanthone Compound

Computational simulation protocols were implemented to execute the in silico evaluations. Molecular docking is an advanced computational algorithm used to model and predict non-covalent interactions between target proteins and small-molecule ligands, effectively mapping binding conformations and thermodynamic binding affinities. As established by Mulyati and Seulina Panjaitan (2021), these advanced computational chemistry architectures have become indispensable components within modern rational drug design and pharmaceutical development, primarily because in silico strategies offer exceptionally resource-efficient and accelerated alternatives to traditional empirical screening. The complete preparation and structure-refinement sequence for the target macrostructures was carried out via the AutoDock Tools suite to facilitate formal protein configuration. Specifically, this computational docking matrix was used to calculate relative binding energies (Sohilait et al., 2017). The structural macromolecular targets investigated in this research comprised three key signaling proteins: Caspase-9 (PDB ID: 1NW9), Tumor Necrosis Factor-alpha (TNF-α, PDB ID: 1TNF), and Estrogen Receptor-alpha (ER-α, PDB ID: 1A52). These receptor crystal structures were isolated, stripped of water molecules and heteroatoms, and structurally optimized using AutoDock Tools, culminating in standardized macrostructures saved in the PDBQT file format. To rigorously validate the docking engine's computational parameters, the co-crystallized endogenous ligands were systematically extracted and redocked into their respective binding pockets. The metrics chosen to validate and quantify these simulation profiles consisted of the structural Root Mean Square Deviation (RMSD) and overall binding affinity scores. Visual mapping of the spatial networks connecting the receptor-binding domains and coordinating amino acid residues was rendered in both 2D and 3D using Biovia Discovery Studio 2025. Furthermore, comprehensive computational modeling of systemic absorption, distribution, metabolism, excretion, and toxicity (ADMET) was completed to map the essential pharmacokinetic and biotransformation profiles required for novel antineoplastic agents, utilizing the online pkCSM predictive platform (https://biosig.lab.uq.edu.au/pkcsm/prediction). Concurrently, the specific toxicological hazards and safety profiles associated with the dimeric xanthone structure were thoroughly profiled utilizing the ProTox II computational toxicology server (https://tox-new.charite.de).

RESULTS AND DISCUSSION

In Vitro Evaluation of the Anticancer Activity of Xanthone Compound

The antineoplastic potency of the dimeric xanthone structure against MCF-7 cells was quantified via the colorimetric MTT metabolic assay. All laboratory trials were performed in independent triplicates (n = 3), and data points are expressed as mean ± standard deviation (SD). The resulting dataset revealed a distinct, direct dose-dependent correlation regarding cellular mortality kinetics. The observed growth inhibition rates across the ascending concentration gradient were calculated at 22.26 ± 0.74%, 32.96 ± 0.64%, 45.45 ± 0.31%, and 69.17 ± 0.27%, respectively. These tight standard deviations, maintaining a relative standard deviation (%RSD) of approximately 3%, demonstrate high experimental reproducibility and robust internal consistency across the biological replicates.

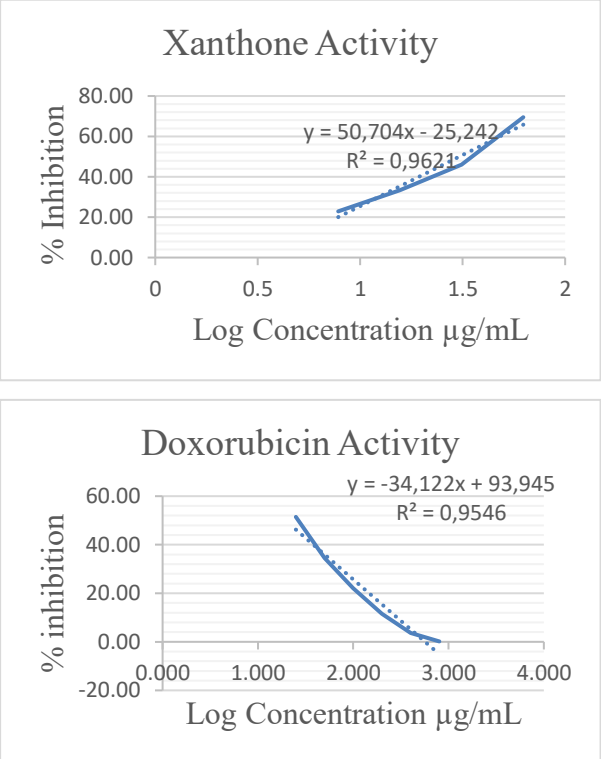

Figure 1. Cytotoxic activity graph against MCF-7 breast cancer cells

The specific half-maximal inhibitory concentration (IC_{50}) computed via linear regression modeling serves as the primary metric for defining overall anticancer efficacy. Figure 1 delineates the comparative metabolic inhibition curves obtained during the MTT trials for both the novel xanthone derivative and the reference chemotherapeutic agent, doxorubicin. The calculated IC_{50} for the dimeric xanthone compound was 30.47 µg/mL, indicating moderate cytotoxicity against ER-positive MCF-7 mammary adenocarcinoma cells. Conversely, the doxorubicin control displayed an IC50 of 19.40 µg/mL, confirming its superior acute cytotoxicity in this in vitro environment.

However, while the synthetic anthracycline exhibits more aggressive cellular destruction, its clinical utility is fundamentally limited by a narrow therapeutic index and documented systemic toxicity to non-malignant tissues. Consequently, the distinct cytotoxic signature of this plant-derived xanthone, paired with its predictable and highly stable dose-response trajectory, highlights its viability as a potentially safer biomimetic lead candidate requiring deeper mechanistic validation.

In Silico Evaluation of the Anticancer Activity of Xanthone Compound

In silico evaluation was performed using molecular docking and ADMET computations to substantiate the potency assessment of these xanthone derivatives toward pivotal oncological target macromolecular entities. The spatial three-dimensional configurations of the biomolecules Caspase9 (Accession: 1NW9), TNF-α (Accession: 1TNF), and ER-α (Accession: 1A52) were retrieved from the Protein Data Bank repository. This computational binding strategy underwent initial validation by redocking co-crystallized endogenous ligands, yielding root-mean-square deviation values below 2 Å, indicating that this predictive protocol remains highly robust and suitable for subsequent exploratory workflows (Table 1). Figures 2 and 3 depict the three-dimensional and two-dimensional graphical representations of these ligand-receptor interaction outcomes, respectively.

The results suggest that the xanthone compound's ability to induce cell death (via Caspase-9), modulate inflammatory pathways (through TNF-α), and interfere with hormone-dependent cancer cell proliferation (through ER-α) may be associated with the cytotoxic effect observed in vitro. Hence, the observed anticancer activity in MCF-7 cells is supported by in silico data.

Table 1. Results of Molecular Docking of Caspase9, TNF-α, ER-α Receptors and Xanthone and Doxorubicin Ligands

Receptors	*Binding Affinity* (kcal/mol)	RMSD (Å)	Amino Acid Residue Interaction
Xanthone Ligand			
Caspase9	-9.7	0.721	Van der Waals: ALA263, CYS303, CYS327, ARG258. Unfavorable Bump: PHE301, HIS302, PRO257, LEU256, LYS328, TYR329. Conventional Hydrogen Bond: CYS300, SER242.
TNF-α	-9.4	3.044	Unfavorable Bump: ARG6, THR7, PRO8, SER9, ASN39, GLU53, GLY54, GLN125. Conventional Hydrogen Bond: ASN39. Pi-Cation: GLU127. Pi-sigma: LEU36. Pi-Alkyl: VAL13, LEU55.
ER- α	-8.8	1.867	Unfavorable Bump: LEU306, ALA307, LEU308, SER309, LEU310, LYS481. Conventional Hydrogen Bond: ASP369

Doxorubicin Ligand			
Caspase9	-8.2	0.096	Unfavorable Bump: LEU256, PRO257, PRO260. Alkyl: ARG258.
TNF-α	-7.3	0.254	Unfavorable Bump: ARG6, THR7, PRO8, SER9. Conventional Hydrogen Bond: SER9. Carbon Hydrogen Bond: GLN125. Pi-Sigma: LEU55 Alkyl: LYS11, LEU36.
ER- α	-8.3	0.019	Unfavorable Bump: LEU306, ALA307, SER309, LEU310, PRO365, GLY366, ASP369. Conventional Hydrogen Bond: LEU308, MET315. Pi-Alkyl: HIS474

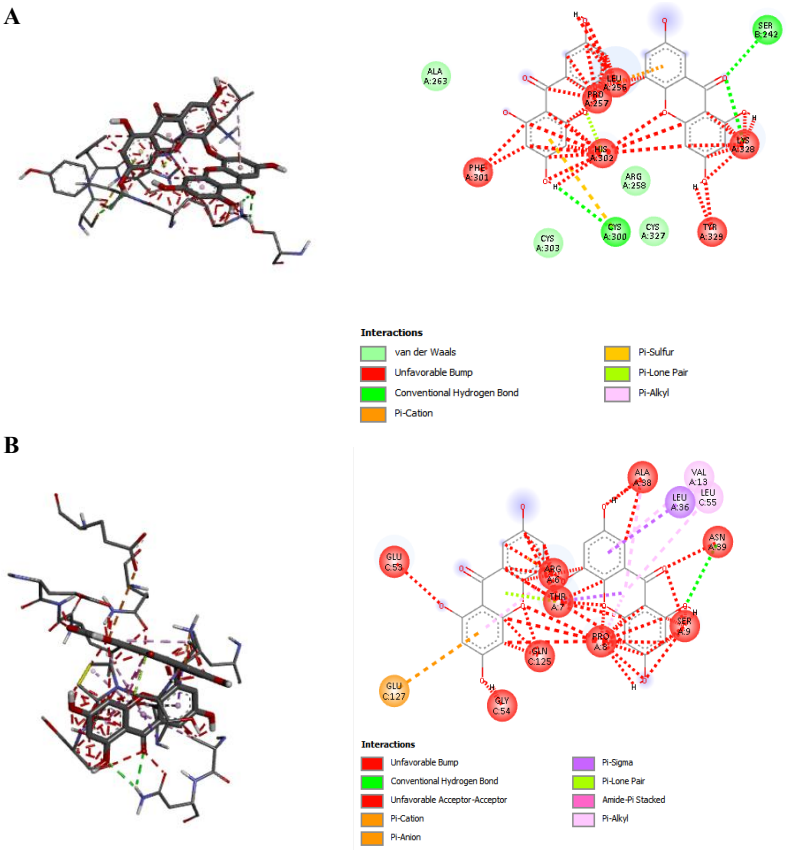

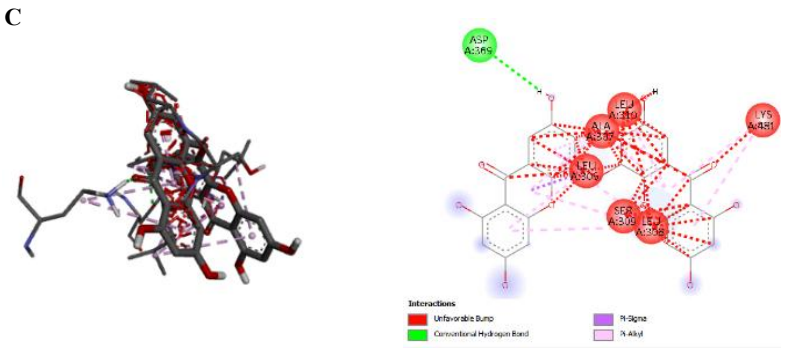

Figure 2. 3D and 2D Visualization of Receptors A. Caspase-9, B. TNF-α, C. ER-α, and the Xanthone Ligand

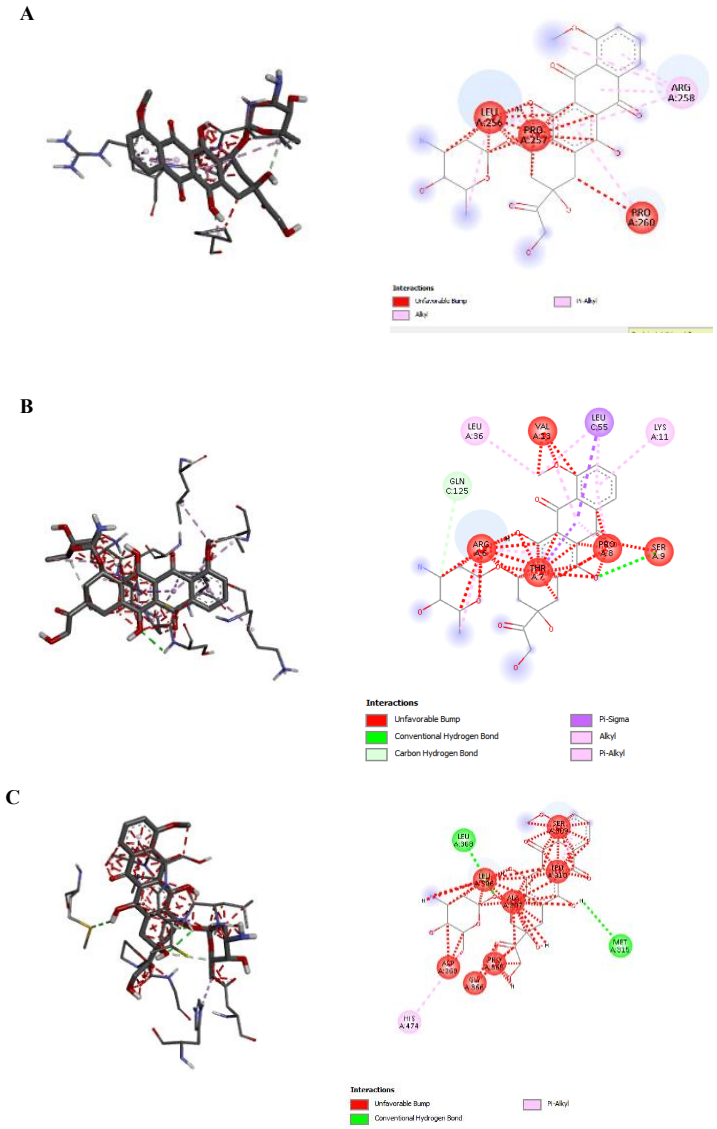

Figure 3. 3D and 2D Visualization of Receptors A). Caspase-9, B). TNF-α, C). ER-α, and The Doxorubicin Ligand

The docking findings show that the xanthone molecule had higher binding affinities than doxorubicin for all receptors tested, with values of -9.7 kcal/mol for caspase-9, -9.4 kcal/mol for TNF-α, and -8.8 kcal/mol for ER-α. One measure of a drug's efficacy is its binding Affinity (Oktavia & Santoso,

2018). A stronger negative affinity results in more stable and long-lasting connections; affinity binding is a measure of the strength of ligand-protein interactions. (Darwati et al., 2021). RMSD values measure the distance between atoms in one conformation relative to those in another. Based on assumptions (Natsir et al., 2024), molecular docking analysis predicts interaction patterns and binding affinities between ligands and target receptors. This simulation generates many ligand-receptor complex conformations, which are assessed using RMSD values to quantify bond-orientation stability. Among the recognised connections are hydrophobic interactions, pi-alkyl interactions, hydrogen bonds, and van der Waals forces. Based on the findings, it seems that the xanthone molecule may form a strong bond with the proteins of interest.

The receptor and ligand affinity binding and root mean squared deviation (RMSD) data are shown in Table 1. The closer the predicted ligand position is to the target, the smaller the RMSD value will be (Lestari, 2015). Computing with an RMSD value less than 2 Å indicates accuracy with fewer errors. The in silico interaction results between the ligand and receptor are not suitable as a reference when the RMSD is 2 Å, indicating significant differences in the computational results. As stated by Ferwadi et al. (2017).

The factors studied include hydrogen-bond networks, van der Waals forces, and hydrophobic interactions between the macromolecular receptor and its ligand to understand the relationship between structural conformation and biological effectiveness. Owing to their ability to span greater distances separating the molecular entities, hydrogen linkages possess greater thermodynamic stability than van der Waals forces (Lodish et al., 2002). Hydrophobic interactions primarily determine the overall structural stability of the ligand-receptor assembly. These specific hydrophobic influences effectively segregate nonpolar amino acid residues away from aqueous environments. Consequently, the ligand and the target protein achieve a highly stabilized spatial immobilization because both hydrophobic and van der Waals interactions become collectively optimized (Lins & Brasseur, 1995).

The xanthone ligand has an RMSD of 0.721 Å and a binding affinity of -9.7 kcal/mol, according to molecular docking data with the Caspase9 receptor. Xanthone establishes contact arrays involving ALA263, CYS303, CYS327, along with ARG258 utilizing van der Waals forces; engages PHE301, HIS302, PRO257, LEU256, LYS328, as well as TYR329 by means of steric clashes; and associates with CYS300 beside SER242 via hydrogen linkages. This core scaffold engages diverse receptor surfaces via distinct mechanisms, including hydrogen bonds involving ASN39, Pi-Cation interactions targeting GLU127, Pi-sigma networks involving LEU36, and Pi-Alkyl interactions involving VAL13 and LEU55, yielding an estimated binding free energy of -9.4 kcal/mol toward the TNF-α macromolecule. The structural deviation value (RMSD) corresponds to 3.044 Å. While simultaneously coordinating with LEU306 alongside ALA307, this derivative registers a binding affinity of -8.8 kcal/mol toward the ER-α target alongside an RMSD calculation of 1.867 Å.

The doxorubicin molecule is immobilized within the Caspase9 active pocket, with an RMSD of 0.096 Å, and displays unfavorable steric overlaps with LEU256, PRO257, and PRO260, as well as alkyl linkages to ARG258. In the TNF-α complex, which includes spatial contacts with ARG6, THR7, PRO8, and SER9 through unfavourable steric hindrances, SER9 and GLN125 through hydrogen bridges, LEU55 through pi-sigma configurations, and LYS11 and LEU36 through alkyl bridges, the binding thermodynamic value is -7.3 kcal/mol, and the RMSD metric is 0.254 Å. The binding Affinity of the ER-α receptor is -8.3 kcal/mol, and its root mean square deviation is 0.019¯. Duloxetine interacts with several proteins via several types of interactions, including pi-alkyl bonds with HIS474, hydrogen bonds with LEU308 and MET315, and unfavourable bump bonds with LEU306, ALA307, SER309, LEU310, PRO365, GLY366, and ASP369.

According to Lipinski et al. (2001), a more stable association between the receptor and the ligand is indicated by a lower binding affinity value. The negative binding affinity values were highest when the xanthone ligand was connected to the Caspase9, TNF-α, and ER-α receptors, as compared to when the doxorubicin ligand was connected to the same receptors. The xanthone ligand forms a stronger and longer-lasting bond with the Caspase9, TNF-α, and ER-α receptors, as indicated by this.

The ligand molecules' binding positions at the protein receptor's binding site are closer to the original conformation when the RMSD is less than 2 Å (Aziz et al., 2022). According to molecular docking experiments, the xanthone ligand exhibits an RMSD of more than 2 Å upon binding to the TNF-α receptor. Given that the doxorubicin ligand has an RMSD value smaller than 2 Å, it may be inferred that the xanthone ligand is less effective and less accurate in targeting the TNF-α receptor. Medication effectiveness cannot be adequately assessed using RMSD values and binding

Affinity alone. Effective drug action occurs upon proper binding of the ligand to its receptor. The strength of the affinity relationship determines the nature and location of the optimal connection. (Hadisoebroto et al., 2025).

Because the naturally existing scaffold Xanthone coordinates within the Caspase9 active pocket utilizing four distinct van der Waals networks beside two hydrogen bridges, TNF-α exhibits a singular hydrogen bridge, one pi-sigma interface, two pi-alkyl linkages (representing hydrophobic forces), plus a solitary pi-cation network (signifying electrostatic stabilization); ER-α demonstrates a single hydrogen bridge. The control molecule, doxorubicin, binds within the Caspase9 binding region via a hydrophobic interaction mediated by a specific alkyl linkage. TNF-α generates two hydrophobic networks, one pi-sigma interface, besides two alkyl linkages; ER-α similarly constructs two hydrophobic networks along with one pi-alkyl interface. This demonstrates that the doxorubicin control lacks the highly robust spatial network configurations observed in the xanthone scaffold, including electrostatic stabilization, hydrophobic contacts, van der Waals networks, and hydrogen bridges. Preliminary estimations, along with the determination of the maximally potent entity, depend on configurations predominantly localized within the binding pocket residues of the target biomolecule (Koentjoro et al., 2020). As stated by Syaqila et al. (2024), the ligand-receptor assembly exhibits superior structural stability and functional potency, driven by hydrophobic forces and van der Waals interactions.

Van der Waals networks, hydrogen bridges, and π-π configurations essentially dictate the molecular-level coordination arrays, thereby optimizing the thermodynamic stability of the ligand-receptor structural assembly. Hydrogen bonding with critical amino acid residues, such as CYS300 and SER242 in Caspase-9, may significantly influence apoptotic pathways. Interactions with residues in TNF-α and ER-α suggest the compound's possible role in inflammatory regulation and oestrogen receptor signalling, respectively.

The findings indicate that the in vitro cytotoxic effect may be linked to the xanthone compound's capacity to cause apoptosis (via Caspase-9), alter inflammatory pathways (by TNF-α), and disrupt hormone-dependent cancer cell growth (via ER-α). Consequently, the in silico findings offer mechanistic validation for the documented anticancer efficacy in MCF-7 cells.

In comparison to doxorubicin, the xanthone molecule demonstrates a superior binding affinity but displays more variability in docking reliability among receptors. Doxorubicin has more consistent RMSD values; nonetheless, its reduced binding Affinity indicates a lesser interaction strength. This underscores a possible trade-off between binding Affinity and conformational stability that must be considered when assessing overall effectiveness.

The prevalence of hydrogen bonds and hydrophobic interactions in xanthone–receptor complexes enhances binding stability and underscores its potential as a multi-target anticancer drug. These findings establish a mechanistic foundation for the cytotoxic effect demonstrated in vitro, specifically through the activation of apoptosis and the regulation of oestrogen receptor signalling.

Using the pkCSM and Protox applications, the ADMET study was conducted to assess the pharmacokinetics of xanthone and doxorubicin compounds. Table 2 presents ADMET results for each chemical when used as an anticancer agent.

Table 2. ADMET Analysis of Xanthone and Doxorubicin Compounds as Anticancer Agents

Pharmacokinetic Parameters	Xanthone	Doxorubicin
Lipinski's Rule		
Molecular weight (g/mol)	502.39	543.53
Log P	4.23	$1.3x10^{-3}$
Hydrogen Bond Donors	6	6
Hydrogen Bond Acceptors	11	12
Absorption		
Water solubility (log mol/L)	-2.89	-3.4

HIA (%)	92.76	50.33
$CaCO_2$ permeability (cm/s)	0.63	0.65
Distribution		
Blood-brain barrier (log BBB)	-2.06	-1.64
Volume of distribution (VDss, human)	-0.72	0.79
CNS permeability	-3.96	-4.35
Metabolism		
CYP2D6 inhibitor	No	No
CYP3A4 inhibitor	No	No
CYP2C9 inhibitor	No	No
Excretion		
Total clearance (mL/min/kg)	0.65	1.05
Renal OCT2 substrate	No	No
Toxycity		
AMES toxicity	No	Yes
Hepatotoxicity	No	No
Neurotoxicity	No	Yes
Cardiotoxicity	No	Yes
Immunotoxicity	No	Yes
Predicted LD_{50} (mg/kg)	3800	205

In the first round of testing, xanthone compounds were evaluated for their potential as oral medicines using Lipinski's Rule of Five. Doxorubicin does not meet three of Lipinski's four criteria; xanthone molecules have better oral bioavailability.

The absorption assessment indicated that the xanthone compound exhibited superior absorption across all dimensions, particularly in Human Intestinal Absorption (HIA), with 92.76% compared to 50.33% for doxorubicin. Conversely, pharmacokinetic data during distribution revealed that the xanthone molecule had challenges in traversing the They showed reduced penetration into the central nervous system and showed increased localisation in blood plasma, which is known as the Blood-Brain Barrier (BBB). Therefore, it is suitable for targeting peripheral cancer cells, including those in breast cancer, and is associated with few neurological side effects.

The likelihood of drug interactions and systemic side effects may be increased, as doxorubicin and xanthone do not inhibit the activity of enzymes responsible for drug metabolism in the liver, as shown in Table 2. Because xanthone is not an OCT2 substrate, it will not interact with other drugs eliminated by the kidneys; rather, it is eliminated via the bile and liver. In contrast to doxorubicin, which exhibits Ames toxicity, neurotoxicity, cardiotoxicity, and immunotoxicity, the xanthone molecule does not exhibit any of these harmful consequences. Compared with the chemical, xanthone's low LD50 of 3800 mg/kg is significant. This toxicity measure signifies the elevated occurrence of doxorubicin adverse effects, including hepatic damage, neurological complications, cardiac failure, and alterations in the immune system.

CONCLUSION

The compound 5,5′-Oxybis (1,3,7-trihydroxy-9H-xanthen-9-one) had a lower cytotoxicity profile than doxorubicin, with an IC50 of 19.40 µg/mL, but showed antineoplastic efficacy against the MCF-7 breast carcinoma line in vitro, with an IC50 of 30.47 µg/mL. Based on ADMET in silico computational mapping, this xanthone scaffold had better pharmacokinetic pathways and safety matrices than doxorubicin (205 mg/kg baseline), and it had no mutagenic, neurotoxic, cardiotoxic, or immunotoxic liabilities. Additionally, it had a significantly higher LD_{50} value at 3800 mg/kg. This xanthone entity displayed optimized binding free energies toward the Caspase9 (−9.7 kcal/mol) and ER-α (−8.8 kcal/mol) target cavities, exceeding those of doxorubicin, which recorded binding free energies toward Caspase9 (−8.2 kcal/mol) and ER-α (−8.3 kcal/mol). The geometric

deviation calculations indicated that the xanthone structure possessed stable docking configurations within the macromolecular receptors Caspase-9 (0.721 Å) and ER-α (1.867 Å), while doxorubicin established coordinates at Caspase-9 (0.096 Å) and ER-α (0.019 Å). A geometric deviation value below 2 Å proves that the spatial localization of these ligands within the biomolecular active pockets mirrors the native crystallographic orientation, thereby validating their potential as effective antineoplastic agents.

SUPPLEMENTARY MATERIALS

Illustration 1.1 displays the ^{1}H-NMR profile corresponding to molecule 1 (600 MHz utilizing acetone-d6), Illustration 1.2 presents the ^{13}C-NMR data characterizing molecule 1 (150 MHz utilizing acetone-*d*6), Illustration 1.3 illustrates the DEPT-135° chart mapping molecule 1 (150 MHz utilizing acetone-d6), Illustration 1.4 depicts the HSQC matrix tracking molecule 1, Illustrations 1.5 and 1.6 show the HMBC networks mapping molecule 1, Illustration 1.7 contains the infrared absorption data of molecule 1 (utilizing KBr matrix), and Illustrations 1.8a,b reveal the HR-TOF-MS mass spectrum identifying molecule 1. In contrast, Illustration 1.9 outlines the TLC chromatogram tracking molecule 1.

ACKNOWLEDGMENT

Prof. Ahmad Faried of the Faculty of Medicine at Padjadjaran University generously provided the breast carcinoma lineages (MCF-7 ATCC-HBT-22TM), and the investigator is deeply indebted to the University of Jambi's 2025 financial allocation scheme (PNBP grant programme), which enabled the smooth progression of this investigative workflow.

REFERENCES

Amir, H., & Murcitro, B. G. (2017). Uji Microtetrazolium (MTT) Ekstrak Metanol Daun *Phaleria macrocarpa* (Scheff.) Boerl terhadap Sel Kanker Payudara MCF. *Alotrop: Jurnal Pendidikan Dan Ilmu Kimia*, *1*(1), 27–32.

Aziz, A., Andrianto, D., & Safithri, M. (2022). Molecular Docking of Bioactive Compounds from Wungu Leaves (*Graptophyllum pictum* (L) Griff) as Tyrosinase Inhibitors. *Indonesian Journal of Pharmaceutical Science and Technology (IJPST)*, *9*(2), 96–107.

Bai, X., Ni, J., Beretov, J., Graham, P., & Li, Y. (2018). Cancer Stem Cells in Breast Cancer Therapeutic Resistance. *Cancer Treatment Reviews*, *69*, 152–163.

Darwati, D., Safitri, A. N., Ambardhani, N., Mayanti, T., Nurlelasari, N., & Kurnia, D. (2021). Effectiveness and Anticancer Activity of A Novel Phenolic Compound from *Garcinia porrecta* against the MCF-7 Breast Cancer Cell Line In Vitro and In Silico. *Drug Design, Development and Therapy*, *15*, 3523–3533.

Ferwadi, G., Gunawan, R., & Astuti, W. (2017). Studi Docking Molekular Senyawa Asam Sinamat dan Derivatnya sebagai Inhibitor Protein 1J4X pada Sel Kanker Serviks. *Jurnal Kimia Mulawarman*, *14*, 85–90.

Hadisoebroto, G., Effendi, S., Al Azzahra, Y., & Sari, L. F. (2025). Analisis Molecular Docking Senyawa Aktif Tanaman Kumis Kucing terhadap Reseptor Carbonic Anhydrase II sebagai Kandidat Obat Antihipertensi. *Journal of Noncommunicable Disease*, *5*(1), 29–52.

Hasanah, U., Budiyanto, R., Triwahyuni, N., Istatik Badi, H., Timur, J., Rungkut Madya No, J., Anyar, G., & Gunung Anyar, K. (2026). Cytotoxicity of Kamandin Saebo *Glossocardia leschenaultii* [Cass.] Veldkamp Extract with Various Solvents on T47D Cells. *Indonesian Journal of Chemical Research*, *13*(3), 235–240.

Hermawan, A., Meiyanto, E., & Susidarti, R. A. (2010). Hesperidin increases the cytotoxic effect of Doxorubicin in MCF-7 Cells. *Majalah Farmasi Indonesia*, *21*(1), 8–17.

Kalkoy, Y., Pattipeilohy, M., Sangur, K., & Mahulette, F. (2025). Pengaruh Ekstrak Kulit Manggis (*Garcinia mangostana* L.) terhadap Kadar Flavonoid dan Kualitas Organoleptik Nata De Soya. *Jurnal Biologi dan Terapan, 11*(2), 237-242.

Koentjoro, M. P., Donastin, A., & P.E., N. (2020). Potensi Senyawa Bioaktif Tanaman Kelor Penghambat Interaksi Angiotensin-Converting Enzyme 2 pada Sindroma SARS-CoV-2. *Jurnal Bioteknologi dan Biosains Indonesia*, *7*(2), 259–270.

Kurniawan, Y. S. (2025). Evaluation of Xanthone and Cinnamoylbenzene as Anticancer Agents for Breast Cancer Cell Lines through In Vitro and In Silico Assays. *Journal of Multidisciplinary Applied Natural Science*, *5*(1), 87–102.

Lestari, T. (2015). Studi Interaksi Senyawa Turunan 1,3-dibenzoiltiourea sebagai Ribonukleotida Reduktase Inhibitor. *Jurnal Farmasi Indonesia*, *7*(3), 163–169.

Lodish, H., Berk, A., Matsudaira, P., Kaiser, C. A., Krieger, M., & Scott, M. P. (2002). *Molecular Cell Biology* (*5th ed*).

https://www.mustafaaltinisik.org.uk/smolecular-cellbiology.pdf

Mohamed, G. A., & Ibrahim, S. R. M. (2022). Garcixanthone E and Garcimangophenone C: New Metabolites from *Garcinia mangostana* and Their Cytotoxic and Alpha Amylase Inhibitory Potential. *Life*, *12*(11).

Mulyati, B., & Seulina Panjaitan, R. (2021). Study of Molecular Docking of Alkaloid Derivative Compounds from Stem Karamunting (*Rhodomyrtus tomentosa*) Against α-Glucosidase Enzymes. *Indonesian Journal of Chemical Research*, *9*(2), 129–136.

Natsir, H., A Arfah, R., Arif, A. R., Nadir, M., Anita, A., Sartika, S., Rahmi, N., & Karimah, A. (2024). In Vitro and In Silico Assessment of Methanol Extract from *Moringa oleifera* Seeds as α-Amylase Inhibitor. *Indonesian Journal of Chemical Research*, *12*(2), 79–88.

Oktavia, D., & Santoso, B. (2018). Interaksi Molekuler Secara 3D Senyawa Terkandung Dalam Kemenyan Jawa dan Adas Bintang Sebagai Inhibitor Protein Sintase 2 dari 3-oksasil-[protein-pembawa-asil] Mycobacterium tuberculosis. *Urecol*.

Safitri, A., Nurlelasari, Mayanti, T., Darwati, & Supratman, U. (2020). 5,5′-Oxybis(1,3,7-trihydroxy-9h-xanthen-9-one): A New Xanthone from the Stem Bark of *Garcinia porrecta* (Clusiaceae). *In MolBank 3*, 1–5. MDPI AG.

Siegel, R. L., Miller, K. D., & Jemal, A. (2017). Cancer Statistics, *CA: A Cancer Journal for Clinicians*, *67*(1), 7–30.

Sohilait, M. R., Dwi Pranowo, H., & Haryadi, W. (2017). *Hypothesis Molecular Docking Analysis of Curcumin Analogues with COX-2*. www.bioinformation.net

Syaqila, C. N., Pebralia, J., Restianingsih, T., & Hrp, N. S. (2024). Molecular Docking Senyawa (8)-Shogaol sebagai Obat Antikanker. *Journal of Pharmacy (JoP)*, *9*(2), 72–76.

Tipaheuw, D., Rahawarin, H., & Tuahuns, A. (2025). *Hubungan Ekspresi Reseptor Estrogen dengan Derajat Histopatologipada Pasien Kanker Payudara di Kota Ambon*. *18*(1).